IL NUOVO CIMENTO **38 C** (2015) 22
DOI 10.1393/ncc/i2015-15022-5

COLLOQUIA: IFAE 2014

Ageing and performance studies of drift chamber prototypes for the MEG II experiment

MARCO VENTURINI on behalf of the MEG COLLABORATION

Scuola Normale Superiore - Piazza dei Cavalieri 7, 56126 Pisa, Italy
INFN, Sezione di Pisa - Largo B. Pontecorvo 3, 56127 Pisa, Italy

received 7 January 2015

Summary. — We present the tests aimed at verifying the proper functioning of the tracking systems of MEG II on small prototypes, estimating the achievable resolutions and evaluating the gain loss experienced by the chamber during its operation.

PACS 29.40.Gx – Tracking and position-sensitive detectors.
PACS 29.40.Cs – Gas-filled counters: ionization chambers, proportional, and avalanche counters.

1. – Introduction

The MEG II experiment will search for the $\mu \to e\gamma$ decay at the Paul Scherrer Institut (PSI) near Zurich, Switzerland. The MEG II tracker is a hyperbolic drift chamber (for a description see [1]), whose drift cells consist of a sense wire surrounded by 8 field wires in an approximate squared shape, with 7 mm side. Sense wires are 20 μm Au-plated W wires, whereas field wires are 40–50 μm Ag-plated Al wires. The detector has a unique volume filled with a low-mass gas mixture of helium and isobutane 85:15. The drift chamber sustains a high flux of Michel positrons, which is expected to be 22 kHz/cm at the hottest sense wires. At a gas gain value of 10^5, this corresponds to a maximum anode current of 10 nA/cm. In three DAQ years the maximal charge per unit wire length will be 0.5 C/cm, therefore a study of its performance under such a high rate is mandatory.

2. – Performance studies

An estimate of the spatial resolution achievable by the MEG II tracker was obtained with a small-scale prototype, consisting of three cells, with the central one having the anode staggered by 500 μm. The wire schematics is implemented on two FR4 Printed Circuit Boards (PCBs), kept at a distance of 20 cm by four rods stretching the wires. The three-cell array is surrounded by guard wires to correctly define the electric field inside the cells. The same wires of the final tracker are used. The prototype was irradiated with a

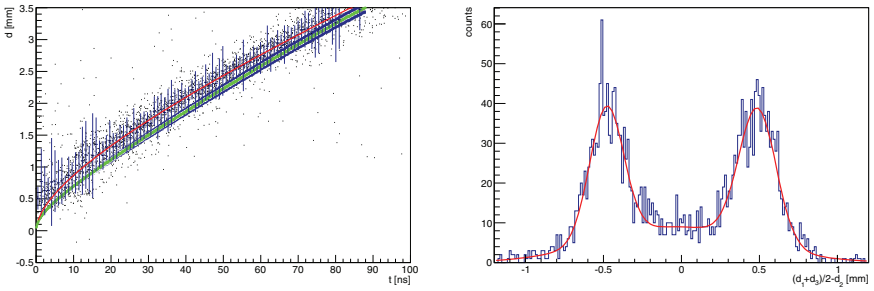

Fig. 1. – On the left drift space-time relation: data (blue), fit (red) and Garfield++ simulation (green). On the right the bimodal distribution for Δ.

^{106}Ru source. From the comparison of drift times in the three cells, we measured the drift space-time relations. We obtained an average drift velocity of $3.5\,\mathrm{cm}/\mu\mathrm{s}$, in satisfactory agreement with Garfield++ simulations. The result is shown in fig. 1. In addition, from the constraint on the three drift distances d_i given by the stagger $\pm\Delta = (d_1 + d_3)/2 - d_2$, an estimate on the resolution was extracted from the bimodal distribution of Δ, shown in fig. 1. The obtained value is $\sigma_d = \sqrt{2/3}\sigma_\Delta \simeq 120\,\mu\mathrm{m}$.

3. – Ageing tests

In order to verify the drift chamber robustness to large amounts of accumulated charge, irradiation tests were performed on two single-cell prototypes. The realization of the prototype is analogous to that of the three-cell one. The sense wire is grounded through a Keithley Sourcemeter 2635A, to measure the current flowing through it. The prototypes were placed in a standard CF100 ultra-high-vacuum steel cross, fed by steel plumbing. All the materials used are known to be clean and to have no considerable effects on wire chamber ageing. X-ray tubes (a Moxtek Magnum X-ray gun and an Oxford Apogee XTF5011) were chosen as irradiating sources: radiation enters and exits the test chamber through two $150\,\mu\mathrm{m}$ Mylar windows, placed at two opposite faces of the cross. An upstream lead collimator defines the size of the irradiated area, while a downstream lead shield damps the X-ray beam, permitting a small fraction of radiation to illuminate a scintillating counter that monitors the beam stability. For quantifying gain loss, we calculate the relative gain loss per unit charge $\mathcal{R}$ [2]. Gain loss evaluation is obtained by measuring the anode current variations under constant irradiation. For reducing the operation time from about 600 days to about a month, a factor 20 of accelerated irradiation should be set in order to reach same charge collection. Two major effects arise with this test methodology. First, it is fundamental to monitor any change of the environmental conditions of the chamber (temperature, pressure...) avoiding possible misidentification of ageing effects. Second, under high radiation levels space charge effects occur and current decreases do not correspond linearly to gain loss. Since the gas system maintains a fixed absolute pressure of the chamber, the former issue can be solved by measuring the gas temperature. Current oscillations induced by temperature variations are removed offline: since gas gain has a power dependence on temperature and pressure with opposite power indices, we measured the behaviour of current as a function of the pressure and obtained the power index (see fig. 2). On the other hand, saturation represents an intrinsic limit on gain loss evaluation in accelerated test. Figure 2 shows anode current

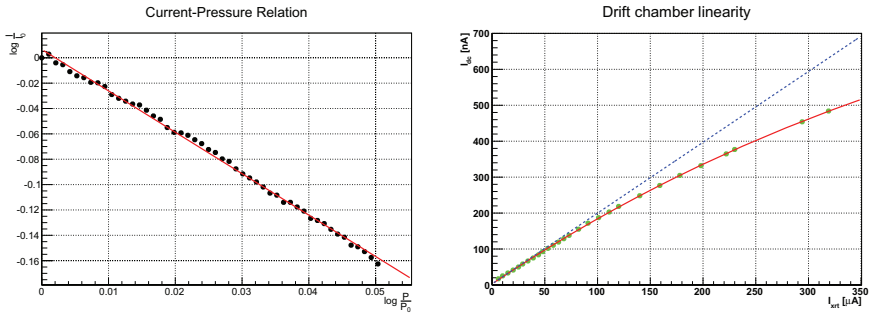

Fig. 2. – Anode current as a function of the gas pressure (left) and as a function of the X-ray tube current (right), measured (solid) and in absence of saturation (dotted).

as a function of the X-ray intensity: deviations from linearity are clearly visible. For describing the curve we adopted a phenomenological expression $I = I^{\mathrm{NS}} \exp(-kI^{\mathrm{NS}})$, where $I^{\mathrm{NS}} = \varepsilon I_{\mathrm{xrt}}$ is the non-saturated current, proportional by definition to the X-ray tube current I_{xrt}. For small deviations from linearity ($kI^{\mathrm{NS}} \ll 1$), we can calculate the non-saturated current as $I^{\mathrm{NS}} = I \exp(kI)$, with the parameter k obtained from the fit in fig. 2. Since the non-saturated current is proportional to the gain, it can be used for calculating $\mathcal{R}$.

4. – Experimental results

4˙1. *Gain loss.* – In the two tests, the ageing rate of the chamber was measured at several working points (reported in detail in table I). No significant slope change corresponds to modification of the chamber working conditions. However a slope change is visible in the normalized gain as a function of the collected charge with Prototype I (fig. 3). The ageing rates measured in the two tests are compatible within 20%:

$$\mathcal{R}_1 = 108 \pm 1\%/(\mathrm{C/cm}),$$

$$\mathcal{R}_2 = 90.9 \pm 0.3\%/(\mathrm{C/cm}).$$

TABLE I. – *Comparison between the operating parameters in the two ageing tests.*

	Prototype I	Prototype II
Anode	25 μm W (Au)	20 μm W (Au)
Cathodes	80 μm W (Au)	80 μm Al (Ag)
Gas mixture	90:10 – 85:15	85:15
Gas flow rate	40 sccm – 5 sccm	15 sccm
Cell gain	$\sim 1 \times 10^4$	$\sim 3 \times 10^4$
Irradiation spot	2.5 cm – 1.8 cm	3 cm
Accelerating factor	$\times 17 - \times 26$	$\times 10 - \times 20$

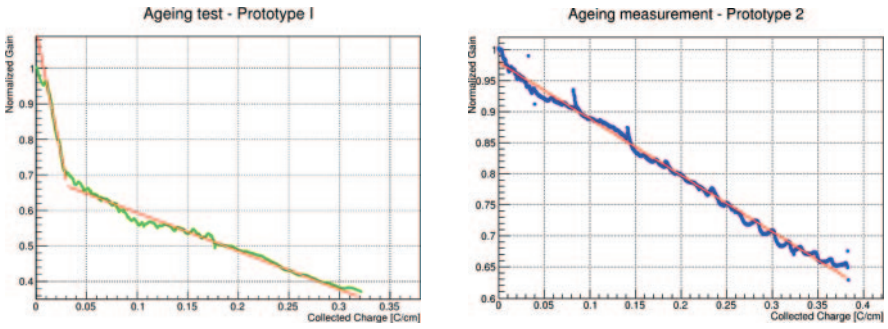

Fig. 3. – Gain decrease as a function of the collected charge for Prototype I (left) and II (right).

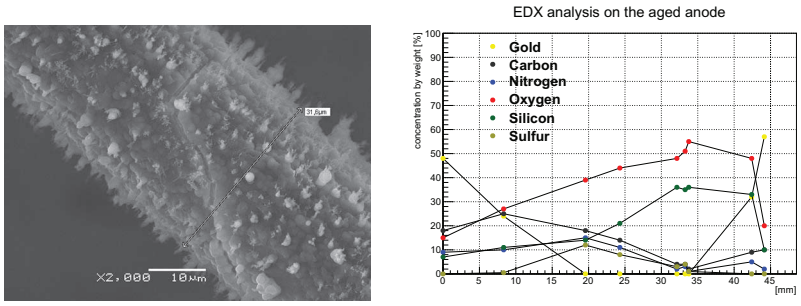

Fig. 4. – SEM image of a portion of aged anode on the left and element concentration along the wire ($x = 0$ is arbitrary) returned by EDX analysis on the right.

4˙2. *SEM/EDX analysis*. – Selected portions of wires were analysed with Scanning Electron Microscopy (SEM) and Energy Dispersive X-ray (EDX) analysis, with the aim of looking for modifications of the wires that can induce gain loss. Cathodes do not present visible modifications, but EDX analysis shows contaminations of carbon, nitrogen, oxygen and silicon, that increase approaching the centre of the irradiated portion of the wire. On the other hand, a uniform coating covers the anode surface (fig. 4). The mean wire diameter is about 30 μm, with extrusions making the peak-to-peak wire size up to about 40 μm (in spite of the original 25 μm). In the proximity of the centre of the wire, in an area extending for about 2 cm, bubbles and whiskers emerge from the coating.

5. – Conclusions

The tests successfully demonstrated the robustness of the chamber to ageing and provided a promising estimate of the single-hit resolution.

REFERENCES

[1] Baldini A. M. *et al.*, arXiv:1301.7225.
[2] Kadyk, John A., *Nucl. Instrum. Methods A*, **300** (1991) 436.